Progress in Additive Manufacturing (2024) 9:1567–1578
https://doi.org/10.1007/s40964-023-00521-9

FULL RESEARCH ARTICLE

Cold spray forming: a novel approach in cold spray additive manufacturing of complex parts using 3D-printed polymer molds

Philipp Kindermann[1] · Maximilian Strasser[1,2] · Martin Wunderer[1] · Ismail Uensal[1] · Max Horn[1] · Christian Seidel[1,2]

Received: 27 June 2023 / Accepted: 25 September 2023 / Published online: 13 October 2023
© The Author(s) 2023

Abstract

The solid-state additive manufacturing (AM) process cold spraying (CS) offers advantageous properties such as melt-free near-net-shape part fabrication and high deposition rates. Compared to other metal-based AM processes such as the powder bed fusion of metals (PBF-LB/M) or directed energy deposition (DED) processes such as laser metal deposition (DED-LB), CS features lower part resolution. One solution to increase the achievable level of detail is spraying onto removable molds. No study exists that investigates the general feasibility and manufacturing boundaries, from which design guidelines could be derived. In this paper, the applicability of material extruded and thermally bonded polymer (MEX-TRB/P) shapes, which is especially suitable for flexible low-cost production of small batches, as molds for cold spray additive manufacturing (CSAM) is investigated. For this purpose, material extruded thermoplastics are examined regarding their suitability for the CS process. Furthermore, geometrical and thus constructive restrictions of this new approach "Cold Spray Forming" (CSF) are analyzed using an industry-relevant use case. It was shown that the feasibility of this approach could be determined by the material value hardness of the sprayed polymer substrates.

Keywords Cold spray forming · Cold spraying · Multi-material · Rapid tooling · Material extrusion of polymers · 3D printing

1 Introduction

Metal additive manufacturing (AM) processes gain further importance, as evidenced by the 10.7% increase in system sales in 2021 [1]. Cold spraying (CS) is a less established process compared with powder bed-based processes (e.g., the laser-based powder bed fusion of metals, PBF-LB/M), but the number of systems sold has also been growing in recent years, as can be seen from the Australian manufacturer Speed3D [1]. The process offers material deposition rates of typical 2–7 kg/h. CS is similar to the directed energy deposition (DED) processes, such as wire arc additive manufacturing (WAAM), which is now in some cases an alternative to conventional manufacturing methods [2]. In this context, structures like walls made up of high strength materials such as 2.4856 (or INCONEL 625®, Alloy 625) are now being successfully built using WAAM [3, 4].

However, CS cannot be clearly assigned to the DED processes, as the sprayed particles remain in a solid state. This characteristic is also the main feature of this process from which the advantages over other comparable technologies are derived: since the particles remain in the solid state, there are no phase changes, and the properties of the feedstock powder can be largely obtained in the sprayed layers. Solely the plastic deformation on impact with the substrate, respectively, the already sprayed particles, leads to an increase in hardness (it is work hardened) of the deposited material as well as a lower oxygen content [5] compared to the feedstock powder. The fact that the particles remain in a solid state and do not have to be melted for bonding makes the process particularly interesting for multi-material applications, as the probability of unfavorable phase formation in the material transition zone is decreased. In this approach, two or more materials are combined in one part to exploit the advantageous properties of both materials.

✉ Philipp Kindermann
philipp.kindermann@igcv.fraunhofer.de

1 Fraunhofer IGCV (Institute for Casting, Composite and Processing Technology), Am Technologiezentrum 10, 86159 Augsburg, Germany

2 Department of Applied Sciences and Mechatronics, University of Applied Sciences Munich, Lothstr. 34, 80335 Munich, Germany

The CS process as an additive manufacturing method (then referred to as "CSAM") is limited in terms of its resolution: the build-up of freestanding geometries is difficult, and the focal point typically has a diameter of 3–10 mm. The layer thickness varies depending on the set powder feed rate, deposition efficiency and gun traverse speed, but usually ranges between 0.1 and 1 mm. Two approaches have been used in industry and research to overcome this limitation and will be described in more detail throughout this paper: first, the use of advanced path planning with compensation strategies to counteract the sloped track edges of the process, and second, the use of metal base parts/molds that either remain in the part or are chemically dissolved or removed by machining.

At NASA, an example of a multi-material part sprayed onto a shape-giving base structure was recently published: a copper alloy GRCop-42 liner manufactured by PBF-LB/M provides a high conductivity for cooling. Afterwards, the nickel alloy "NASA HR-1" is sprayed as a structural jacket to obtain a high strength to withstand the pressure during subsequent operation of the final combustion engine [6].

However, the combined materials do not have to be metals in CS. Polymers and metals can be combined, for example, as an insulator and conductor for electric applications. In this paper, the combination of metal powder and polymer substrates is studied for a specific purpose, namely to encounter the aforementioned low resolution of the process, using polymer molds. These are to be manufactured using the 3D-printing method "material extrusion of polymers with thermal reaction bonding" (MEX-TRB/P), to achieve a high degree of geometric freedom. This process is often referred to as fused filament fabrication (FFF). After spraying, the molds must be removed, comparable to the lost-mold process in casting technology. For that, the polymers processed by means of MEX-TRB/P must also be qualified for CS.

Due to a higher achievable complexity, parts like the PBF-LB/M-manufactured liner mentioned by Gradl et al. [6] could then also be produced almost completely by the cold spray forming (CSF) method presented in this study. This approach adds several degrees of freedom and design capabilities compared to conventional metallization processes, such as electroplating for example. This is because, unlike most coating processes, CSF also allows variations in the volume of the applied material on the mold, by adjusting the spray parameters (e.g., feedrate or gun traverse speed). The term cold spray forming itself was first used by Wong et al. to generally describe an early approach of CSAM [7]. Since CSAM as well as its nomenclature have evolved and in accordance with conventional spray forming [8, 9], it is suggested to use the term CSF for CSAM on molds or mandrels to create near-net-shape parts.

2 State of the art and research gap

In the state of the art, CS per se and on polymers are briefly discussed and, in addition, the MEX-TRB/P process is briefly described.

2.1 Cold spraying process and additive approaches

CS uses kinetic energy for the deposition process. Therefore, the particle velocity is a crucial parameter. It must exceed the so-called critical velocity. Below this material-dependent level, no material is applied, but erosion is occurring. The particle velocity is mainly influenced by

- Carrier gas type
- Pressure of the total gas flow
- Temperature of the total gas flow
- Design of the used nozzle
- Morphology and density of the sprayed particles

As soon as the powder particles hit the substrate material, which is metal for the majority of applications, they deform plastically and create dense layers with the subsequently impinging particles. The bonding mechanisms are a combination of metallic bonding and mechanical interlocking and are currently still the subject of research and scientific discourse [10–13].

The sprayed-on tracks typically have a Gaussian profile. Particles at the edge of the nozzle are slower than in its center, so that the application efficiency already varies across the width of the exit opening [14]. The width of the tracks (typically $3-8$ mm) depends on the outlet opening as well as the distance of the nozzle from the substrate. The Gaussian distribution continues through the built-up layers, so without appropriate build-up strategies, the material deposition will peak at one point, where no further deposition is possible.

Wu et al. [15] as well Pattison et al. [16] have already presented strategies to compensate falling edges. The approach of Wu et al. allows the build-up of walls perpendicular to the substrate plane. Here, the robot-guided gun and thus the nozzle are tilted towards the substrate at a defined angle and offset to the track center in to compensate the Gaussian profile by angled spraying. Despite the ingenuity of this approach, it has drawbacks, which is why it is not suitable for all part shapes and thus use cases:

- *Overspray*: during the tilted spraying of the slanted edges, the impact angle is not 90° and thus not optimal.
- *Resolution*: the thinnest buildable structure results from the minimal track width, which in turn depends on the

diameter of the nozzle opening and the standoff distance, plus the two compensation tracks on each side.

- *Path planning*: the two compensation paths on each side of the sprayed tracks must be executed at a tilted angle. This results in practical difficulties for robot path planning, such as passing through singularities or just in increased programming effort for complex shaped bodies or overhangs.

In the case of the aforementioned example of the rocket engine, it does not seem feasible to use this approach due to its shape, which contains thin walls and overhangs.

Another approach to the realization of more complex structures is CS onto base parts or molds. Despite its potential, little research exists on this approach. Examples can be found in Cavaliere [17], Lenling et al. [18], as well as in one patent of Dindl et al. [19]. In Lenling et al. steel tubes were successfully fabricated with an Al alloy core, which was subsequently dissolved with a NaOH solution [18]. The patent by Dindl et al. describes the production of gun barrel liners, which are also to be realized with a solvable core [19]. In an article by Yin et al. in Cavaliere's book [17], the use of molds is reviewed with some examples such as a bracket. Figure 1 shows the function principle of this approach.

Furthermore, when spraying on molds, care must be taken to ensure that their geometrical features do not lead to cracked surface layers. This is particularly the case for angles that lead to an unacceptably strong deviation from the ideal impact angle. Figure 2 shows the problem.

So far, the approaches have been limited to metal molds. With increasing part complexity, these are costly to manufacture and difficult or nearly impossible to remove in the case of undercuts. Thus, the use of additively manufactured solvable polymer molds seems to be a promising approach.

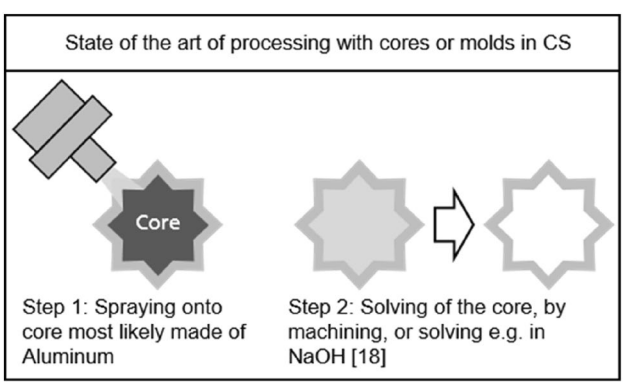

Fig. 1 Schematic representation of the state of the art of spraying onto solvable cores

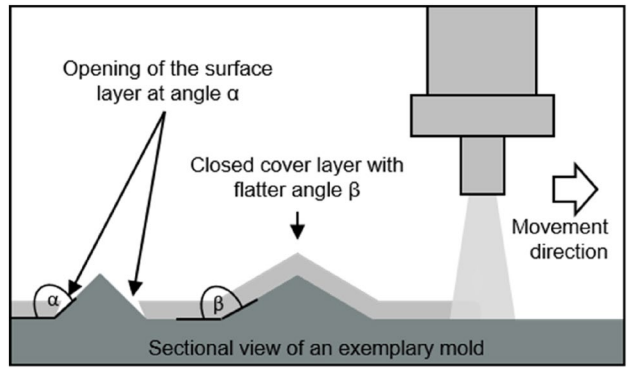

Fig. 2 Problem representation of cracked surface layers

2.2 Rapid tooling

According to the DIN EN ISO/ASTM 52900 [20] standard, the term "rapid tooling" describes the application of additive manufacturing for the production of tools to reduce lead times compared to conventional tool production. Therefore, this term is accurate for the application of the MEX-TRB/P process described in this paper.

The functional principle of MEX-TRB/P is that a thermoplastic polymer filament is conveyed through a heated nozzle. The melted string is then applied to a build plate, or the previous layer, according to the contour of the respective layer of the build job. The process is limited to thermoplastics. Due to its simplicity, low investment and operating costs, the process is attracting a high number of users in both the industrial and private sectors. Materials such as acrylonitrile butadiene styrene (ABS) or polylactic acid (PLA) can already be processed on entry-level 3D printers. High-performance thermoplastics such as polyether ether ketone (PEEK), on the other hand, require technically more sophisticated printers that have a heated build chamber, to achieve sufficient part qualities.

The use for MEX-TRB/P for the rapid tooling of molds for CSF is promising—despite the limitation of the process to thermoplastics—since these are more suitable as substrates for CS than thermosetting polymers. That is because thermoplastics are susceptible to thermal softening—just like metals. This occurs at temperatures exceeding the glass transition temperature of the thermoplastic polymer [21].

2.3 Cold spraying on polymer substrates

Due to the low process temperatures in CS, it is generally possible to deposit metals on thermoplastic polymers (cf. previous section). So far, the metallization of these polymers has mainly been pursued with the aim of depositing a conductive layer, e.g., by Chen et al. [22] who coated PEEK with pure copper (Cu).

Several other examples for polymer metallization already exist in the literature, although the results are heterogeneous. The review of 13 publications from recent years [21, 33] shows that 59% of the analyzed combinations of metal powder and polymer substrates were successfully sprayed. In some publications, several combinations of metal powder and polymer substrates are analyzed so that their number exceeds the number of literature references. According to the authors' definition, a material deposition is only considered successful if it exceeds more than one sprayed layer. Often only a particle embedment occurs as described by Che et al. [21]. This means that solely individual particles have penetrated the substrate surface and locked in there.

However, in 88% of the successfully sprayed combinations of metal powder and polymer substrates, adjusted parameters were used for the initial layers. This means, for example, that Cu was sprayed onto the polymer substrate at a lower pressure and temperature, compared to a metallic substrate, to avoid erosion. The use of adapted parameters, which are reduced compared to CS of metals, therefore, seems to be crucial for the successful spraying on polymers.

Furthermore, it must be noted that all polymers considered in the publications are conventional sheet materials, thus not 3D printed.

2.4 Problem statement and novel approach

All identified publications regarding CS on molds have in common that, on the one hand, *metallic* and *conventional* machined molds are used and, on the other hand, the aimed geometries of the sprayed parts are *relatively simple*.

The CSF method presented in this paper is intended to be both more cost-effective by the use of 3D-printed thermoplastic polymers and to allow greater flexibility in the molds produced and thus greater complexity in the sprayed parts as well as easier removal of the mold.

To achieve this objective, thermoplastic polymers for MEX-TRB/P must be identified to provide a suitable basis as a substrate/mold for CSF.

3 Materials and methods

The approach is structured as follows: after a pre-selection of relevant polymers (filaments) and a metallic powder for CS, the material deposition on the respective substrate was investigated, whereby specially designed test setups were used. Subsequently, process-related restrictions were determined based on a 3D-printed Test Artifact. Finally, the results were validated by manufacturing an industrially relevant use case.

3.1 Cold spraying equipment and metal powder

The experiments were carried out on a high-pressure CS system Plasma Giken PCS-100. The powder feeder is a POG-2030 from the same manufacturer. Nitrogen 5.0 was used as the propellant gas. The tests were all carried out with a WC-Co nozzle to prevent degradation of its internal geometry and thus a loss of particle velocity.

Spherical Cu powder from the manufacturer M4P material solutions GmbH with a nominal particle size distribution (PSD) of − 45/ + 15 µm was used. The PSD was additionally determined using the software Fiji (ImageJ) for a graphical analysis of the Scanning Electron Microscope (SEM). The SEM was a Hitachi TM3030Plus. The result is shown in Table 1. In addition, micrographs were obtained using an Olympus BX53M optical light microscope.

The material was selected, because it offers a wide parameter window and, in particular, can be sprayed successfully at low pressures and temperatures. In addition, preliminary tests had shown that Cu combines well with other materials, which makes it a suitable material for the investigation of the entirely new approach. Figure 3 shows two images of the used Cu powder. The particles are mostly spherical but a few satellites were observed on their surfaces.

3.2 Polymer selection for the rapid tooling of cold spray molds

Eleven 3D-printed polymers were used as a substrate for spraying. Furthermore, a control group consisting of four conventionally manufactured polymer plates was additionally tested.

The samples were fabricated on two different MEX-TRB/P-printers: For PEEK an Intamsys FUNMAT HT Enhanced was used, which offers a heated enclosure and build plate as well as sufficient nozzle temperatures of up to 450 °C. The remaining materials were fabricated on a Zortrax M300. All samples were printed with 100% infill. The examined filaments and the associated data are listed in Table 2.

The materials were selected according to the following aspects: establishment as a filament material and thus printability (e.g., PLA), hardness (e.g., PC-ABS), temperature resistance (e.g., PEEK), price (e.g., ABS), and solubility (e.g., Polyvinyl acetate, PVA). The selection intends to cover a material spectrum as wide as possible. Since the intended application is the fabrication of lost molds, particular emphasis was placed on solvable polymers, such as PVA, which can be easily dissolved with water. ABS also offers a simple solvability

Table 1 M4P Cu particle size distribution

Material	d10,2 in µm	d50,2 in µm	d90,2 in µm
M4P pure Cu	16.0	21.0	43.7

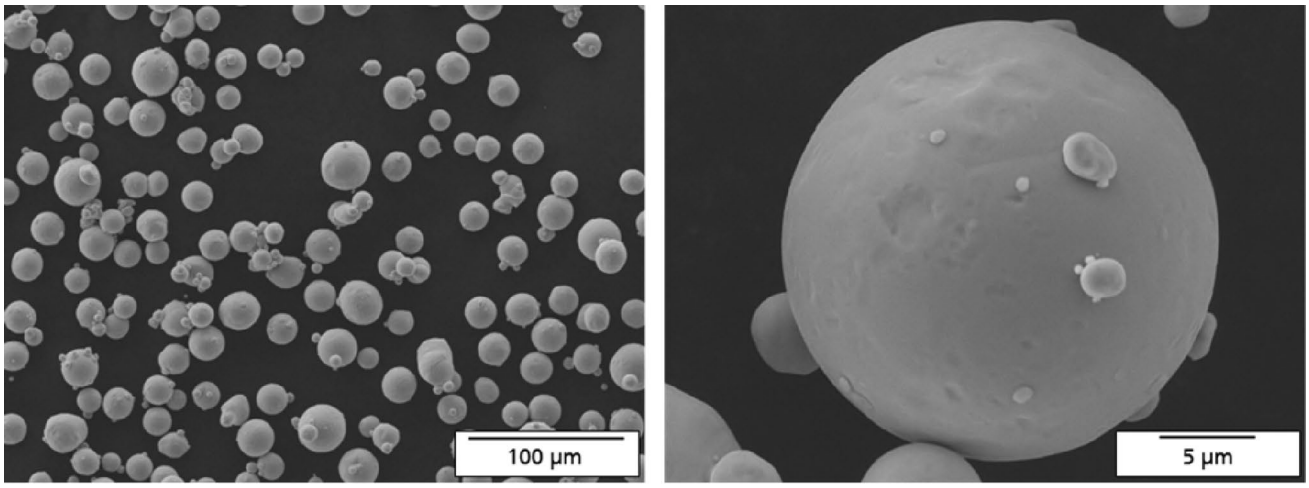

Fig. 3 SEM images of the used pure Cu powder

Table 2 Overview of analyzed polymers

Polymer type	Supplier reference	Supplier	Glass transition temperature in °C	Specified shore D hardness as specified by the supplier at room temperature	Measured shore D hardness (3D printed) at 21° C	Filament cost in €/kg
Acrylonitrile butadiene styrene (ABS)	Z-ABS	Zortrax	107.89	69.2	69.13	39.37
Acrylonitrile butadiene styrene (ABS)	Z-ULTRA	Zortrax	106.4	73.4	71.47	61.78
Acrylonitrile butadiene styrene (ABS) + Polycarbonate (PC)	Z-PCABS	Zortrax	118	N/A	77.83	62.37
High Impact Polystyrene (HIPS)	Z-HIPS	Zortrax	98.68	73.2	68.13	61.87
Polyvinyl acetate (PVA)	HELIOS Support	Form Futura	N/A	N/A	73.17	129.67
Polyvinyl acetate (PVA)	ATLAS Support	Form Futura	60.2	N/A	59.6	113
Polyvinyl acetate (PVA)	AquaSolve	Form Futura	60.2	N/A	71	105.67
Polyvinyl acetate (PVA)	Z-Support	Zortrax	N/A	N/A	56.47	199.99
Acrylonitrile butadiene styrene + (x-%) carbon fiber	ABS-Carbon	Kimya	95	72.2	76.47	114
Polyether ether ketone (PEEK)	PEEK	Intamsys	143	85	85.50	719.98

using acetone. Some materials can only be dissolved using rather aggressive chemicals: e.g., PEEK can only be dissolved completely in concentrated sulfuric and nitric acid.

The PEEK specimens also had to be heat treated after printing. This was carried out according to the specifications of the filament manufacturer Intamsys.

The surface roughness of the printed PEEK specimens (of the later sprayed top surface) was additionally determined and resulted in an average Sa of 52.1 µm over an area of 150 mm^2. These measurements were performed on a Keyence VK-X3000 laser scanning microscope.

Since the hardness of the substrate has a major influence in CS, especially with deviating material pairings [34], (coating material is different from substrate) this parameter was investigated for all 3D-printed samples. The measurement of the Shore D hardness was carried out with a Sauter HDD 100–1 test instrument, mounted on a lever test rig Sauter TI-DL. These measurements were performed at room temperature of 21 °C and at an elevated temperature of 100 °C. For this purpose, the specimens were heated in an oven and tested immediately after taking them out. Figure 4 shows the determined Shore D hardness values at 21 °C and

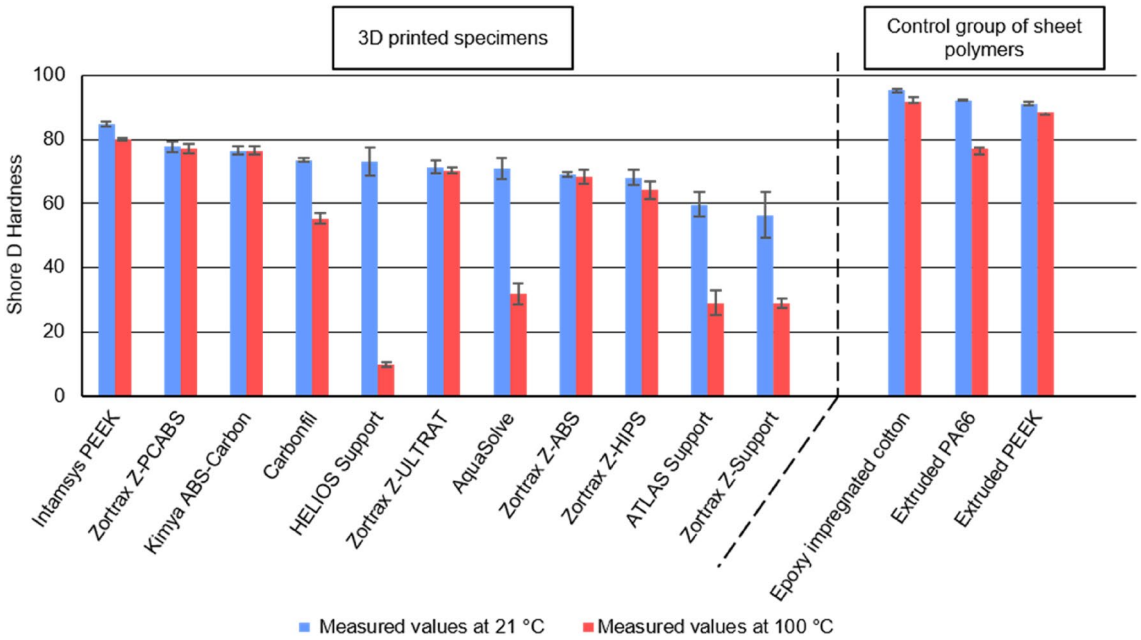

Fig. 4 Measured shore D hardness at 21 ℃ and 100 °C

at 100 °C. The three materials shown on the right side of the diagram are the control group consisting of commercially available sheet polymers.

3.3 Polymer qualification for cold spray forming

In order to ensure a high degree of comparability and a time-efficient test procedure, a carrier plate was milled from aluminum alloy EN-AW 5083. This setup allows mounting of up to 45 samples. Five parameter sets were tested on three materials per experiment. Therefore, 15 samples were required of each polymer to obtain three comparable specimens for each parameter set. For each set, single tracks with three passes (= layers) were sprayed. Figure 5 shows a carrier plate with positioned samples. Before spraying, all samples were cleaned, to ensure a grease-free surface.

The chosen parameters are listed in Table 3. The process window for Cu is rather large, especially when considering the temperatures of the exiting gas stream at the standoff distance (SOD), which differ within a spectrum of 100 °C. The temperatures of the exiting gas stream were measured with a data logger MCR-4TC of Japanese company T&D and type K sheath thermocouples. Only the gun temperature and pressure were varied. The powder gas flowrate—an important parameter as proven in [35] was set constant at 300 standard liters per minute (SLM). The feedrate was set on 3 rpm, which resulted in 87.6 g/s for the Cu powder used and the powder gas flowrate applied. A SOD of 30 mm was chosen. The traverse speed of the robot was set to 100 mm/s.

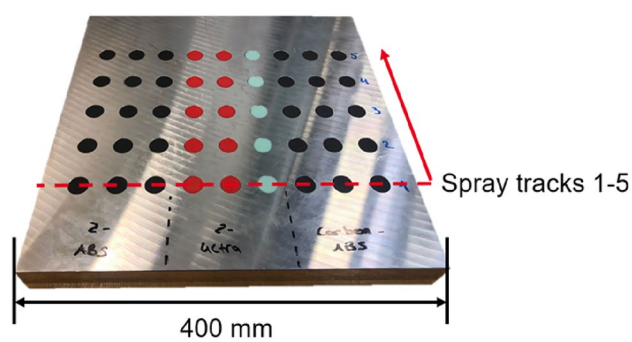

Fig. 5 Carrier plate for efficient testing

Table 3 Applied parameters

Track	1	2	3	4	5
Gun temperature in °C	300	300	400	500	500
Gun pressure in Mpa	3	5	4	3	5
Resulting total gas stream temperature in °C	90.91	131.23	139.01	139.48	196.26

3.4 Determination of the constructive limits of 3D-printed molds

A test part, inspired by the published NIST artifact [36], was designed using the computer-aided design software Siemens NX12 to examine the achievable level of detail of the

sprayed molds. Figure 6 shows the designed Test Artifact with dimensions 120 mm × 100 mm × 6 mm (W × L × H). The limits at which the surface layer is no longer closed, and thus the geometric boundary conditions are exceeded, are to be determined. Furthermore, the featured design methods of fillets and chamfers are to be tested to determine their suitability for enabling closed cover layers in CS.

The Test Artifact is intended in particular to determine the angular transition above which the material coating and its top layer is no longer closed (cf. state of the art) and thus unusable. This was evaluated by qualitative investigation of the following criteria: material deposition beyond the initial coating, and existence of cracks on the top layer.

When spraying the Test Artifact, 40 layers were applied with the initial coating parameters of Track 5 (cf. Table 3) and 20 additional layers with metal powder/metal substrate parameters for Cu on Cu. Thus, the pressure was adjusted to 4 MPa and the temperature to 850 °C, whereas the other values were maintained. The single tracks of the layers were sprayed adjacent to each other at a distance of 5 mm. Here, a path planning strategy already presented in Ref. [37] was used: according to this strategy, the reversal points, and thus the areas of reduced robot speed caused by deceleration and acceleration during turning, are not placed on top of each other, but are offset from each other. In this way, excessive material build-up in the corners is avoided.

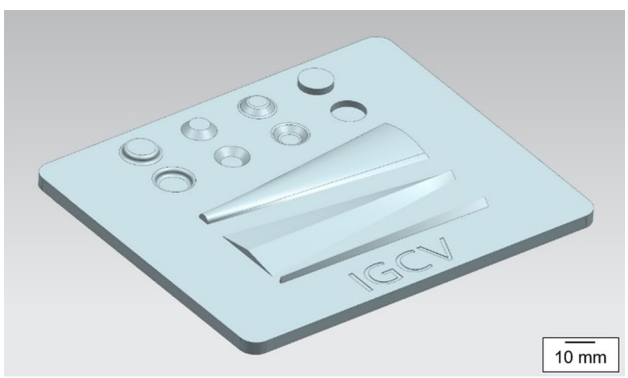

Fig. 6 Designed test artifact to examine the limits of CS on polymers

4 Results and discussion

4.1 Material deposition

A material deposition that went beyond embedding one particle layer could only be achieved with 3D-printed PEEK and conventional PEEK sheet material. All five sets of parameters applied resulted in material deposition on the surrounding aluminum substrate.

For all other polymers, only the initially impinging particles could be embedded in the substrate. As mentioned in the state of the art, this effect has already been described and does not represent a CS material deposition [21].

The particles were shot into the substrate, but they cannot induce plastic deformation in the particles hitting the substrate subsequently. Figure 7 shows three printed specimen pins with only an initial material deposition and no further build-up. The remaining seven pin types of the unsuccessfully coated materials look almost identical and are, therefore, not featured.

The embedding of the particles during the initial deposition can be seen under the microscope. The particles have penetrated the substrate, but have retained their sphericity. The micrograph in Fig. 8 shows a cross-section through a specimen pin made of ABS processed by MEX-TRB/P.

The absence of plastic deformation of the particles results in the impossibility of material deposition by means of CS. In order to obtain an indication of the sprayability of the polymers as a substrate, the hardness (Shore D) was

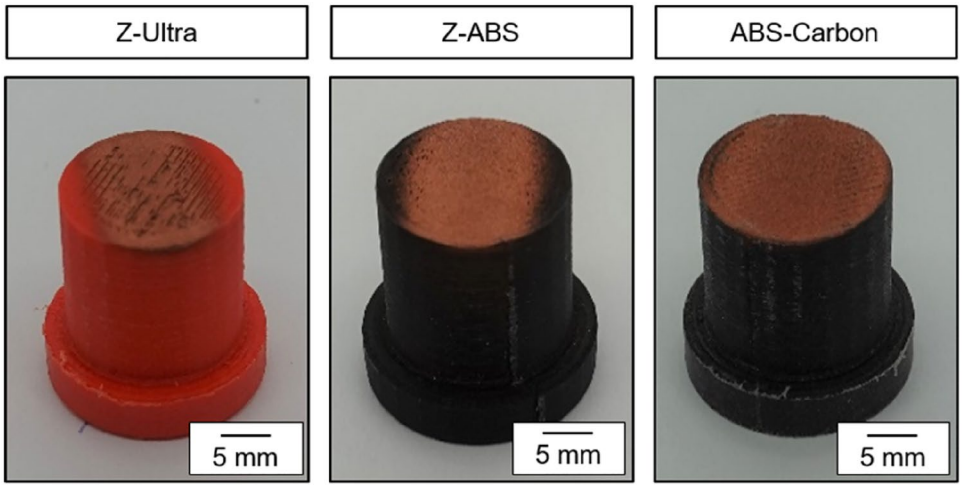

Fig. 7 Three examples of only initial coated specimen pins with no further material deposition

used. This material parameter, as already mentioned, has a great influence in CS: On the one hand, the hardness of the substrate must be sufficiently high to be able to induce plastic deformation of the particles. On the other hand, it must not be too high so that initial penetration of the particles remains possible. When looking at the hardness of all printed polymers (cf. Fig. 4), it is noticeable that the only successfully coated material, PEEK, has the highest value of about 85.5 Shore D within the extruded materials.

In the control group of specimens, all materials exhibit a similarly high or even higher hardness than PEEK. However, it was not possible to generate a material deposition on any of these materials. The explanation for the epoxy impregnated cotton laminate has already been provided by Che et al. [21]: this belongs to the thermosets and not to the thermoplastic materials. The latter shows similar behavior to metals in CS, as they soften due to the temperature introduced in the process, thus allowing penetration of the particles. Thermosets, on the other hand, exhibit brittle behavior and do not soften under the influence of heat, making them unsuitable for CS.

Nylon 66 (hereafter PA66) is also a thermoplastic and could not be coated despite its high Shore D hardness. The explanation for this lies in the severe decrease of the Shore D hardness at elevated temperatures: it decreases from 92.3 at room temperature to about 77 at a temperature of 100 °C. In comparison, the 3D-printed PEEK only drops from a Shore D hardness of 84.9 (at 21 °C) to 80.2 (at 100 °C). Table 3 shows that even at the lowest selected parameter set, the temperatures reach almost 100 °C, so the hardness has already decreased significantly for this specific polymer.

The PEEK substrate does not appear to be subject to degradation, but this aspect will not be considered further here, as the condition of the polymers as a mold to be dissolved is of secondary importance.

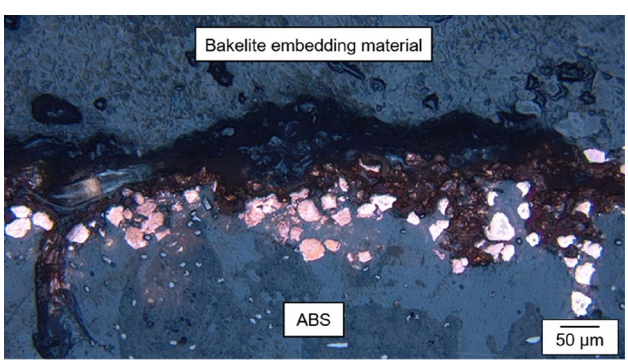

Fig. 8 Micrograph of the embedded particles in ABS

4.2 Model presentation of the polymer spray behavior

In order to categorize the described effects, a model representation was worked out for this purpose, which shows the processes of particles impacting the substrate surface. The models are shown in Fig. 9. The previously described non-induced plastic deformation of the impacting particles appears to be due to insufficient bearing of the initially embedded particles.

4.3 Cold spray forming process restrictions

Three Test Artifacts were successfully sprayed, and shown in Fig. 10.

The geometric feature of the angular transition indicates that from a flatter angle greater than 150° (cf. Fig. 2) the surface layer becomes closed, as indicated by the white arrows in a.

The holes and the standing pins with chamfers and fillets could not be oversprayed with a closed top layer on any Test Artifact. Therefore, no statement can be made about their different effects.

The letters in the Test Artifacts were evenly sprayed. In b, it can be seen that these were also well reproduced in the subsequently detached plate as a negative. Since the Test Artifact has no undercuts, the material application could be detached by hand without having to dissolve the PEEK mold. The surface structure of the individually deposited polymer strings, which is typical for MEX-TRB/P, is also clearly visible in the detached material deposition.

However, the surface layers are not completely closed in some areas: in addition to distributed defects in the form of holes, the deposited material cracked off at several positions. Here, the Test Artifacts show differences in direct comparison with each other. The cause for the deviating material application quality is assumed to be the fluctuating print quality. These qualitative differences occurred despite the use of the same filament and the same printing parameters. The most common defect here is the under-extrusion of the material as shown in c), which leads to an incomplete, yet filigree material deposition with CS.

4.4 Validation of cold spray forming using an industry-relevant use case

As already mentioned in the introduction using the example of the NASA rocket liner, CS is used in particular in the aerospace industry. A base body of a rocket liner was, therefore, built in this context to validate the findings for an industry-relevant use case. To achieve this purpose, a PEEK

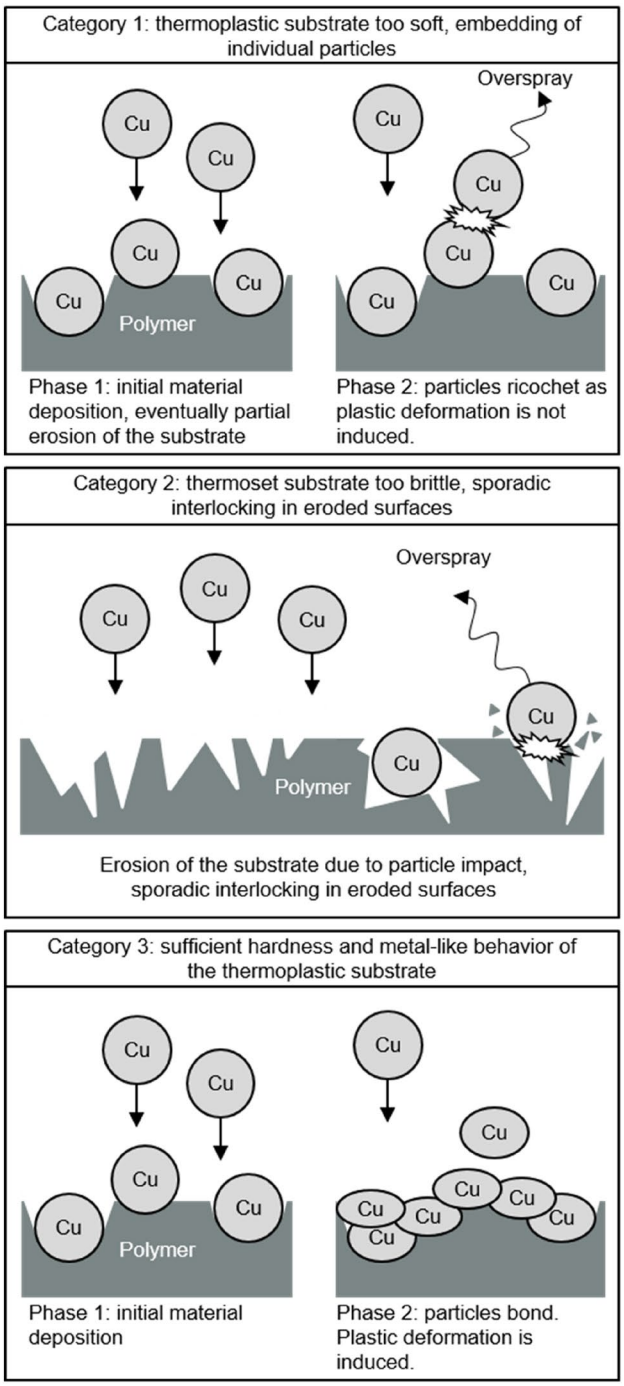

Fig. 9 Model representation of the three identified effects in spraying of polymers

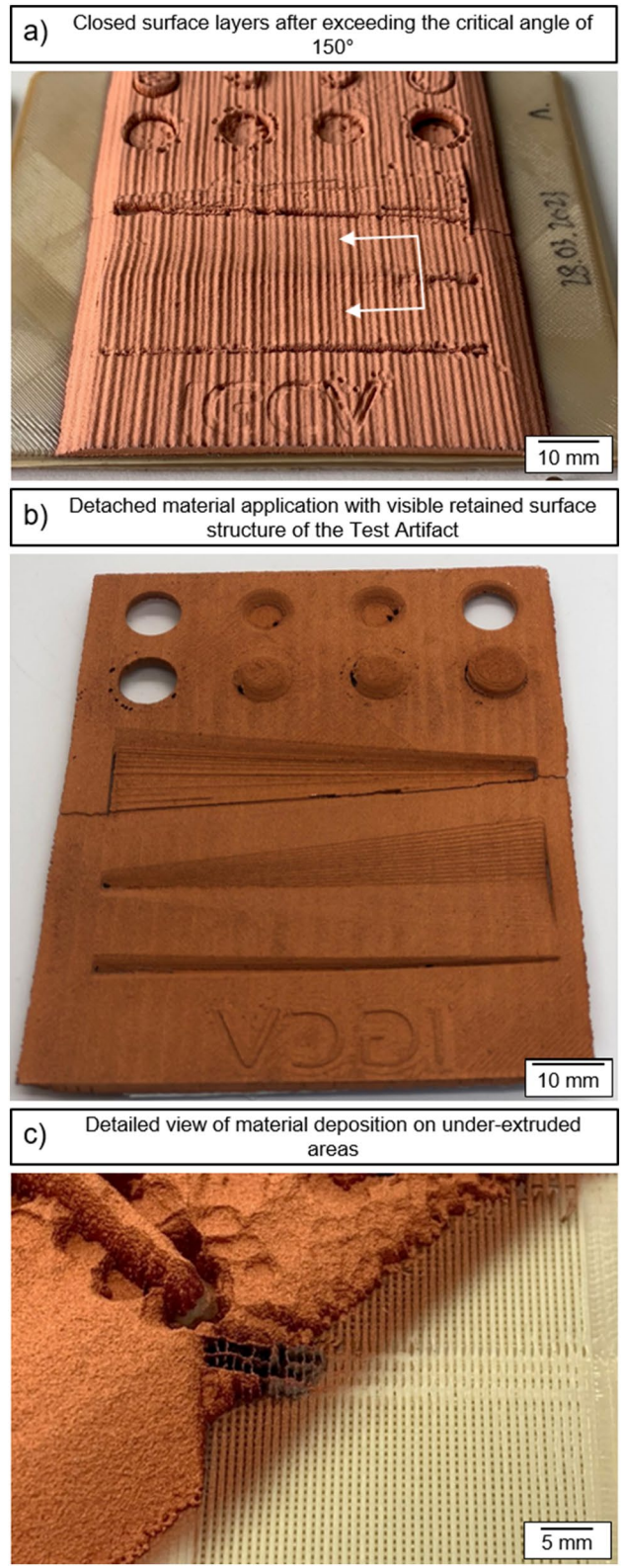

Fig. 10 Sprayed Test Artifacts

mold was 3D printed and sprayed, considering the results presented so far. Figure 11 shows the finished liner with a height of approx. 200 mm and a base diameter of 135 mm.

The rapid tooling of the PEEK mold via MEX-TRB/P took about 28 h, while the actual CSF process took only about 55 min. The mold was clamped upright on a rotary table. The gun was moved up and down according to the

Fig. 11 Sprayed rocket liner on PEEK mold

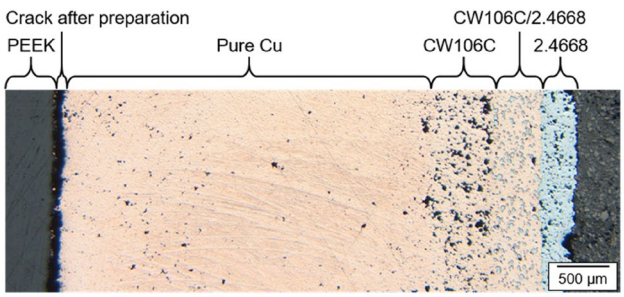

Fig. 12 Micrograph of the sprayed layers on the rocket liner with the multi-material transition

shape of the mold, maintaining a constant SOD of 30 mm. The robot path was programmed so that the rotation speed of the rotary table varied dynamically, depending on the position of the gun. This made it possible to achieve a constant tangential speed of 115 mm/s and thus a constant material thickness. For this purpose, the rotational speeds of the table were varied between 144.8°/s for the smallest diameter of the mold and 105.4°/s for its largest diameter. Several materials were sprayed: Cu, CW106C, a composite of CW106C/2.4668 (or INCONEL 718®, Alloy 718) and 2.4668. The material transition can be taken from Fig. 12. The initial focus was to apply a uniform crack-free Cu deposition as a base layer for the subsequent materials. This was successfully applied. In the subsequent layers of the other materials, an increasing porosity becomes apparent, which in this context can be attributed to non-ideal parameters. Apart from this, the demonstrator showed the potential of CSF also for other materials and their combinations. To dissolve the PEEK, either acids, as described previously in Sect. 3, or a heat treatment (which is necessary anyway for 2.4668), can be applied, in which the PEEK is molten out.

5 Conclusion and outlook

It has been shown that the use of molds produced by rapid tooling via MEX-TRB/P for CS is not only possible, but also a promising novel approach to overcome the limited level of details of this process. The term "Cold Spray Forming" or short "CSF" was introduced.

Except for PEEK, material deposition of Cu could not be achieved for any of the investigated polymers. The explanation for this lies in the sufficient hardness of PEEK, especially under elevated process temperatures, which exceeds the hardness of the other thermoplastic materials.

Despite the fluctuating print quality of the developed Test Artifacts, three reliable conclusions could be drawn regarding the geometric limits:

- The print quality has a major influence on the quality of the subsequently sprayed layers; even small areas of under-extrusion lead to cracks that propagate through to the top layer of the build-up.
- The critical angle for the transition to geometrical features is approximately 150°. Smaller and thus steeper transitions lead to cracks in the surface layer.
- It became apparent that the surface texture of the printed shapes continued into the sprayed-on layers, resulting in the possibility to spray even finer elements than the lettering provided in the presented Test Artifacts.

The findings were validated based on a use case, which could be sprayed with a completely closed surface.

To advance the approach of CSF further, the geometric limits of the sprayability must be determined more precisely, the chemical and/or thermal dissolution of the molds needs to be validated, and the quality of MEX-TRB/P fabricated PEEK parts has to be improved. Furthermore, CSF can be combined with existing additive strategies for cold spray (such as those of Wu et al. [15]). In addition, design methods to derive molds from finished part design have to be developed.

Supplementary Information The online version contains supplementary material available at https://doi.org/10.1007/s40964-023-00521-9.

Acknowledgements The authors are thankful for the research possibilities enabled by the Bavarian Government and the Bavarian Ministry of Economic Affairs, Energy and Technology by funding the "Multi-Materialzentrum Augsburg". Furthermore, the authors would like to thank Erik Maidhof and Kurt Hartmann for their support while conducting the experiments.

Funding Open Access funding enabled and organized by Projekt DEAL.

Data availability The authors state that the experimental data of the study is included in the publication. If the raw data is needed in a different format, it is available upon request from the corresponding author.

Declarations

Conflict of interest The authors state that there are no conflict of interest with the content of this manuscript.

Open Access This article is licensed under a Creative Commons Attribution 4.0 International License, which permits use, sharing, adaptation, distribution and reproduction in any medium or format, as long as you give appropriate credit to the original author(s) and the source, provide a link to the Creative Commons licence, and indicate if changes were made. The images or other third party material in this article are included in the article's Creative Commons licence, unless indicated otherwise in a credit line to the material. If material is not included in the article's Creative Commons licence and your intended use is not permitted by statutory regulation or exceeds the permitted use, you will need to obtain permission directly from the copyright holder. To view a copy of this licence, visit http://creativecommons.org/licenses/by/4.0/.

References

1. Wohlers T, Campbell RI, Diegel O, Kowen J, Mostow N, Fidan I (2022) Wohlers report 2022: 3D printing and additive manufacturing global state of the industry. Wohlers Associates ASTM International, Washington
2. Çam G (2022) Prospects of producing aluminum parts by wire arc additive manufacturing (WAAM). Mater Today Proc. https://doi.org/10.1016/j.matpr.2022.02.137
3. Günen A, Gürol U, Koçak M, Çam G (2023) Investigation into the influence of boronizing on the wear behavior of additively manufactured Inconel 625 alloy at elevated temperature. Springer Nature, New York. https://doi.org/10.1007/s40964-023-00398-8
4. Ceritbinmez F, Günen A, Gürol U, Çam G (2023) A comparative study on drillability of Inconel 625 alloy fabricated by wire arc additive manufacturing. J Manuf Process. https://doi.org/10.1016/j.jmapro.2023.01.072
5. Champagne VK (2007) The cold spray materials deposition process: fundamentals and applications. Woodhead, Cambridge, Boca Raton
6. Gradl PR, Teasley TW, Protz CS, Garcia MB, Ellis D, Kantzos C (2021) Advancing GRCop-based bimetallic additive manufacturing to optimize component design and applications for liquid rocket engines. AIAA propulsion and energy 2021 forum. American Institute of Aeronautics and Astronautics, Reston, Virginia
7. Wong W, Irissou E, Vo P, Sone M, Bernier F, Legoux JG, Fukanuma H, Yue S (2013) Cold spray forming of inconel 718. J Therm Spray Tech 22:413–421. https://doi.org/10.1007/s11666-012-9827-1
8. DeGarmo EP, Black JT, Kohser RA (2003) Materials and processes in manufacturing, 9th edn. Wiley, Hoboken
9. Bauckhage K (1995) Sprühkompaktieren als Alternative zu Guß und Pulvermetallurgie. Spektrum der Wissenschaft 47:108
10. Assadi H, Gärtner F, Klassen T, Kreye H (2019) Comment on adiabatic shear instability is not necessary for adhesion in cold spray. Scripta Mater. https://doi.org/10.1016/j.scriptamat.2018.10.036
11. Assadi H, Gärtner F, Stoltenhoff T, Kreye H (2003) Bonding mechanism in cold gas spraying. Acta Mater 51:4379–4394. https://doi.org/10.1016/S1359-6454(03)00274-X
12. Hassani-Gangaraj M, Veysset D, Champagne VK, Nelson KA, Schuh CA (2018) Adiabatic shear instability is not necessary for adhesion in cold spray. Acta Mater 158:430–439. https://doi.org/10.1016/j.actamat.2018.07.065
13. Hassani-Gangaraj M, Veysset D, Champagne VK, Nelson KA, Schuh CA (2019) Response to comment on "adiabatic shear instability is not necessary for adhesion in cold spray." Scripta Mater 162:515–519. https://doi.org/10.1016/j.scriptamat.2018.12.015
14. Kotoban D, Grigoriev S, Okunkova A, Sova A (2017) Influence of a shape of single track on deposition efficiency of 316L stainless steel powder in cold spray. Surf Coat Technol 309:951–958. https://doi.org/10.1016/j.surfcoat.2016.10.052
15. Wu H, Xie X, Liu M, Verdy C, Zhang Y, Liao H, Deng S (2020) Stable layer-building strategy to enhance cold-spray-based additive manufacturing. Addit Manuf 35:101356. https://doi.org/10.1016/j.addma.2020.101356
16. Pattison J, Celotto S, Morgan R, Bray M, O'Neill W (2007) Cold gas dynamic manufacturing: a non-thermal approach to freeform fabrication. Int J Mach Tools Manuf 47:627–634. https://doi.org/10.1016/j.ijmachtools.2006.05.001
17. Cavaliere P (ed) (2018) Cold-spray coatings: recent trends and future perspectives. Springer, Cham
18. Lenling M, Yeom H, Maier B, Johnson G, Dabney T, Graham J, Hosemann P, Hoelzer D, Maloy S, Sridharan K (2019) Manufacturing oxide dispersion-strengthened (ODS) steel fuel cladding tubes using the cold spray process. JOM 71:2868–2873. https://doi.org/10.1007/s11837-019-03582-w
19. Dindl F, Nardi A, Champagne VK, Klecka M, Jacob A (2019) Cold spray methods for manufacturing gun barrels. US10281227 (B1) 2019-05-07
20. DIN EN ISO/ASTM 52900:2022-03, Additive Fertigung Grundlagen Terminologie (ISO/ASTM 52900:2021); Deutsche Fassung EN_ISO/ASTM 52900:2021. Beuth Verlag GmbH, Berlin
21. Che H, Chu X, Vo P, Yue S (2018) Metallization of various polymers by cold spray. J Therm Spray Tech 27:169–178. https://doi.org/10.1007/s11666-017-0663-1
22. Chen C, Xie X, Xie Y, Yan X, Huang C, Deng S, Ren Z, Liao H (2018) Metallization of polyether ether ketone (PEEK) by copper coating via cold spray. Surf Coat Technol 342:209–219. https://doi.org/10.1016/j.surfcoat.2018.02.087
23. Che H, Vo P, Yue S (2017) Metallization of carbon fibre reinforced polymers by cold spray. Surf Coat Technol 313:236–247. https://doi.org/10.1016/j.surfcoat.2017.01.083
24. Ganesan A, Yamada M, Fukumoto M (2013) Cold spray coating deposition mechanism on the thermoplastic and thermosetting polymer substrates. J Therm Spray Tech 22:1275–1282. https://doi.org/10.1007/s11666-013-9984-x
25. Ganesan A, Affi J, Yamada M, Fukumoto M (2012) Bonding behavior studies of cold sprayed copper coating on the PVC polymer substrate. Surf Coat Technol 207:262–269. https://doi.org/10.1016/j.surfcoat.2012.06.086
26. Lupoi R, O'Neill W (2010) Deposition of metallic coatings on polymer surfaces using cold spray. Surf Coat Technol 205:2167–2173. https://doi.org/10.1016/j.surfcoat.2010.08.128
27. Lupoi R, Stenson C, McDonnell KA, Dowling DP, Ahearne E (2016) Antifouling coatings made with cold spray onto polymers: process characterization. CIRP Ann 65:545–548. https://doi.org/10.1016/j.cirp.2016.04.015
28. Małachowska A, Winnicki M, Konat Ł, Piwowarczyk T, Pawłowski L, Ambroziak A, Stachowicz M (2017) Possibility of spraying of copper coatings on polyamide 6 with low pressure cold spray method. Surf Coat Technol 318:82–89. https://doi.org/10.1016/j.surfcoat.2017.02.001

29. Rokni MR, Feng P, Widener CA, Nutt SR (2019) Depositing Al-based metallic coatings onto polymer substrates by cold spray. J Therm Spray Tech 28:1699–1708. https://doi.org/10.1007/s11666-019-00911-y
30. Tsai JT, Akin S, Zhou F, Bahr DF, Jun MBG (2021) Establishing a cold spray particle deposition window on polymer substrate. J Therm Spray Tech 30:1069–1080. https://doi.org/10.1007/s11666-021-01179-x
31. Viscusi A, Durante M, Astarita A, Boccarusso L, Carrino L, Perna AS (2020) Experimental evaluation of metallic coating on polymer by cold spray. Proc Manuf 47:761–765. https://doi.org/10.1016/j.promfg.2020.04.232
32. Viscusi A, Perna AS, Astarita A, Boccarusso L, Caraviello A, Carrino L, Della Gatta R, Durante M, Sansone R (2019) Experimental study of cold sprayed metallic coatings on thermoplastic matrix composites. KEM 813:68–73. https://doi.org/10.4028/www.scientific.net/KEM.813.68
33. Zhou XL, Chen AF, Liu JC, Wu XK, Zhang JS (2011) Preparation of metallic coatings on polymer matrix composites by cold spray. Surf Coat Technol 206:132–136. https://doi.org/10.1016/j.surfcoat.2011.07.005
34. Assadi H, Kreye H, Gärtner F, Klassen T (2016) Cold spraying—a materials perspective. Acta Mater 116:382–407. https://doi.org/10.1016/j.actamat.2016.06.034
35. Kindermann P, Wunderer M, Binder M, Arnhold J, Ünsal I, Seidel C, Schlick G (2022) Investigation of the Influence of the powder gas flow rate onto the build quality of cold spray copper alloy parts. 16th CIRP Conference on Intelligent Computation in Manufacturing Engineering '22, Italy.
36. Moylan S, Slotwinski J, Cooke A, Jurrens K, Donmez M (2012) Proposal for a standardized test artifact for additive manufacturing machines and processes. Proceedings of the 23rd International Solid Free Form Symposium—An Additive Manufacturing Conference. 23 902–920
37. Kindermann P, Straßer M, Binder M, Wunderer M, Ünsal I, Seidel C (2021) Fabrication of sensor-integrated parts using cold spray additive manufacturing. Euro PM2021

Publisher's Note Springer Nature remains neutral with regard to jurisdictional claims in published maps and institutional affiliations.